Earth and Planetary Science Letters 384 (2013) 81–87

Contents lists available at ScienceDirect

Earth and Planetary Science Letters

www.elsevier.com/locate/epsl

Generation of talc in the mantle wedge and its role in subduction dynamics in central Mexico

YoungHee Kim [a,*], Robert W. Clayton [b], Paul D. Asimow [b], Jennifer M. Jackson [b]

[a] School of Earth and Environmental Sciences, Seoul National University, Seoul 151-742, South Korea
[b] Division of Geological and Planetary Sciences, California Institute of Technology, Pasadena, CA 91125, USA

ARTICLE INFO

Article history:
Received 13 August 2013
Received in revised form 3 October 2013
Accepted 4 October 2013
Available online 27 October 2013
Editor: P. Shearer

Keywords:
subduction
talc
serpentine
receiver function
mantle wedge
P-to-S velocity ratio

ABSTRACT

Geophysical evidence shows the presence of low-seismic velocity material at the surface of slabs in subduction zones. In the central Mexican subduction zone this appears as a thin (~4 km) low-velocity zone that absorbs nearly all of the strain. The P-to-S velocity ratio as a function of S wave velocity distinguishes among the various candidate hydrous (low-strength) minerals; the thin layer in the flat-slab region is most consistent with a layer showing enrichment in talc overlying normal MORB-like gabbro. Based on available thermodynamic data for equilibria for talc, its generation at the trench is nearly impossible, and hence we propose it originates from the mantle wedge during the slab flattening process coupled with trench rollback. The evolution of this low-strength zone has important implications for the dynamics of the slab-flattening process as well as the geochemistry of the mantle wedge and arc in central Mexico.

1. Introduction

The presence of low-velocity material that extends to depths of ~150 km with a thickness of 2–8 km along the slab–mantle interface has been detected in a number of modern subduction zones using teleseisms (Abers, 2000, 2005; Abers et al., 2003). Such low-velocity layers have been interpreted as either hydrated oceanic crust due to subduction of hydrous materials and subsequent up-dip fluid transport (Abers, 2000), or mélange material composed dominantly of chlorite and talc on top of the subducting oceanic crust (Marschall and Schumacher, 2012). The strength of the slab–mantle interface greatly influences interplate frictional behavior and may thus control the extent to which convergent motions between the slab and the overriding plate are accommodated by earthquake slip, post-seismic deformation, or interseismic creep (Lay and Bilek, 2007).

Recent imaging based on the teleseismic converted phase in Cascadia have been able to resolve a few km thick low-velocity, high P-to-S velocity ratio (V_p/V_s) channel at the upper portion of subducted crust (Audet et al., 2009; Hansen et al., 2012). Reported high V_p/V_s values (2.3–2.8) have been used to argue for fluid-filled porosity of 2.7–4.0% with the fluid under near-lithostatic pressure at a depth of less than 35 km (Audet et al., 2009; Peacock et al., 2011). Also, in Nankai, southwestern Japan, a zone of high V_p/V_s (1.9–1.95) is imaged beneath the plate boundary at a depth of ~25–30 km (Kodaira et al., 2004; Shelly et al., 2006). The high pore fluid pressures appear to be an important and necessary factor, which can explain low seismic velocities, and the promotion of slow slip earthquakes and tremors, both observed in shallow subduction environments such as Cascadia (Audet et al., 2009; Peacock et al., 2011), Nankai (Kodaira et al., 2004; Shelly et al., 2006), and also in central Mexico (Song et al., 2009; Kim et al., 2010; Song and Kim, 2012). However, at deeper depths anhydrous minerals may play a role in reducing the strength of the interface.

Central Mexico is an ideal place to examine seismic velocity variations along the crust–slab and slab–mantle interfaces and within subducting oceanic crust because: first, there is an available high-quality dense-array dataset (Middle American Subduction Experiment, MASE (MASE, 2007); Fig. 1; Perez-Campos et al., 2008) oriented along the subduction direction (Fig. 1). Second, the top of the oceanic Cocos plate beneath Mexico is cooler because of the lack of a thick insulating sedimentary cover (Currie et al., 2002). Third, a single down-dip profile in our study region (black solid line, Fig. 1) exhibits shallow-flat-steep progression of slab dip angles (Fig. 2A; Perez-Campos et al., 2008; Kim et al., 2010) with progression in slip behavior distributed with depth (Kostoglodov et al., 2010). Fourth, the subducting Cocos plate horizontally underplates the North American plate for ~325 km from the trench

* Corresponding author.
E-mail addresses: younghkim@snu.ac.kr (Y. Kim), clay@gps.caltech.edu (R.W. Clayton), asimow@gps.caltech.edu (P.D. Asimow), Jackson@gps.caltech.edu (J.M. Jackson).

0012-821X/$ – see front matter
http://dx.doi.org/10.1016/j.epsl.2013.10.006

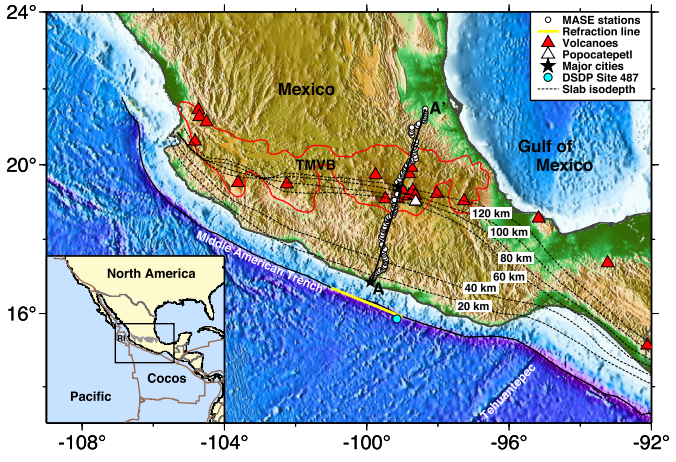

Fig. 1. Topographic-bathymetric map of the central Mexico subduction zone with 100 broadband seismic stations (open circles) used in the analysis. Lower-left inset illustrates the regional tectonic framework. Red line in the North American continent delineates Trans-Mexican Volcanic Belt (TMVB). Thin black dashed lines are slab depth isocontours at 20 km intervals based on Wadati-Benioff seismicity and receiver functions (Perez-Campos et al., 2008; Kim et al., 2010). The surface projection (A–A′; oriented 16° east of north) is shown as a black line in the North American continent. Two black stars indicate major cities located close to the MASE (Acapulco at the Pacific coast and Mexico City within the TMVB). A yellow line at the trench shows station locations from 1954 Acapulco Trench Expedition seismic-refraction survey (Shor and Fisher, 1961). DSDP Site 487 is located 10 km seaward of the axis of the trench off Mexico (Watkins et al., 1982).

with no intervening asthenosphere at a depth of ~45 km (Fig. 2; Perez-Campos et al., 2008; Kim et al., 2010).

Of the flat subduction regions worldwide, the subduction system in central Mexico is unique because of the absence of the asthenosphere above the 250 km-long horizontal Cocos slab. Proposed mechanisms for the flat subduction are (1) the subduction of the young lithosphere or thickened crust in a form of an aseismic ridge due to buoyancy (Gutscher et al., 2000), (2) curvature of the margin (Gephart, 1994), (3) absolute motion of the overriding plate (Lallemand et al., 2005), and (4) structure of the overriding plate (Perez-Gussinye et al., 2008; Manea et al. 2013a, 2013b). There is no apparent cause such as the presence of oceanic impactor (Skinner and Clayton, 2010) or thickened continental (cratonic) lithosphere (Perez-Gussinye et al., 2008; Manea et al. 2013a, 2013b) that can influence the subduction angle in central Mexico.

Mode converted phases suggest the presence of a low-strength, low-velocity layer between the subducting oceanic lithosphere and the overriding plate, which completely decouples the overriding plate from the subducting oceanic lithosphere in the flat-slab region (Song et al., 2009; Kim et al., 2010). Numerical models require a low-viscosity channel atop the subducting crust to support the current flat-slab configuration (Manea and Gurnis, 2007), suggesting that the uppermost horizontal layer of the oceanic crust in central Mexico, observed to have notably low seismic velocity (Song et al., 2009; Kim et al., 2010; Song and Kim, 2012), provides the necessary low-viscosity channel.

Location of the low seismic velocities coincides with the observed slow-slip patch extending from Acapulco to ~100 km inland along the MASE profile (Fig. 2A; Larson et al., 2007; Song et al., 2009). By modeling tangential-component receiver functions, a combination of clay minerals like talc and high pore fluid pressure in the layer is found to be necessary for the shallow part of the subduction system (Song and Kim, 2012). However, the influence of the pore pressure on seismic velocities is expected to decrease with depth (Christensen 1984; 1989) and is likely insignif-

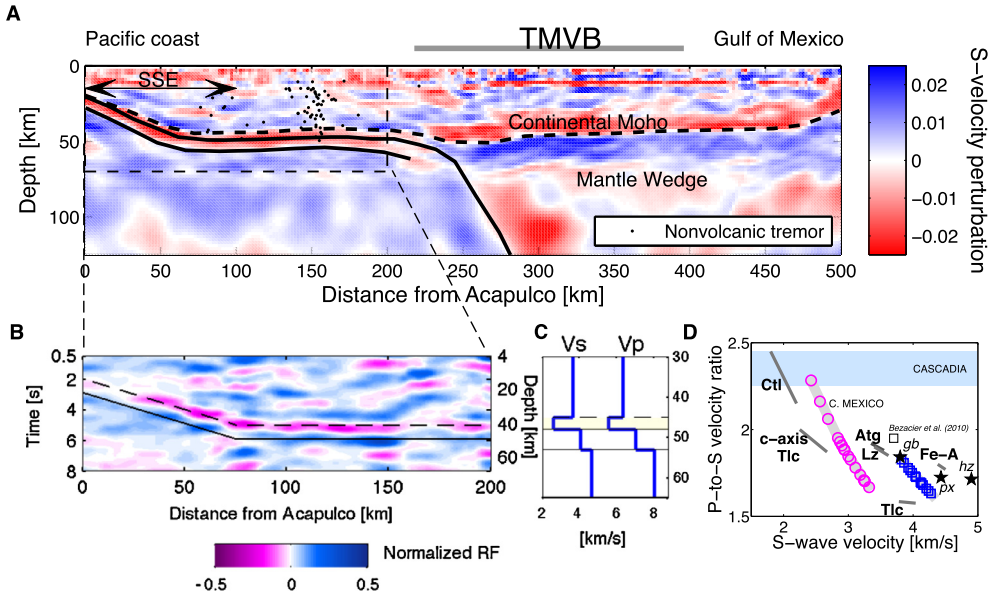

Fig. 2. Seismic observations and candidate mineral phases. (A) Migrated scattered-wave dV_s/V_s image for 500 km transect (A-A′ in Fig. 1; modified from Kim et al., 2012a; method details are presented in Kim et al., 2012a). Red to blue color scale represents slower to faster V_s perturbations relative to the 1-D model. The top and bottom interfaces of the oceanic crust are shown as black lines. Relocated seismicity (Pardo and Suárez, 1995), non-volcanic tremors (Payero et al., 2008) and the extent of the 2006 slow slip event (SSE; Kostoglodov et al., 2010) are also plotted. (B) Receiver function image from Acapulco to a point 200 km from the coast, showing the shallow-to-flat oceanic crust (modified from Kim et al., 2010; method details are in Kim et al., 2010). The negative and positive receiver function conversions at the bottom interfaces of the fore-arc crust and oceanic crust are shown as dashed and solid lines, respectively. (C) V_p and V_s profiles for the flat-slab region down to a depth of 70 km with the same line scheme as A and B. The layer with anomalously low-velocities is highlighted in light yellow. (D) Calculated V_p/V_s ratio versus V_s at the depth of the flat slab and a range of likely temperatures (500–800 °C) for candidate hydrated phases (gray lines) and rock types (black stars) (modified from Kim et al., 2010). The data points near the plate interface are shown as magenta circles for central Mexico. For comparison, the data points for Cascadia (Peacock et al., 2011) are also plotted and shown as light blue. The points for randomly oriented talc and *c*-axis oriented talc are from Mainprice et al. (2008), and those for different rock types from Christensen and Salisbury (1975). The points for antigorite are taken from 30° incident to basal plane. Abbreviation of rock names: gb – gabbro, px – pyroxenite, hz – harzburgite. Abbreviation of mineral phases: Ctl – chrysotile, Tlc – talc, Atg – antigorite (Bezacier et al., 2010), Lz – lizardite, Fe-A – Fe-bearing phase A. The data point shown as a square indicated a value computed for S-wave velocity at a 30° incidence angle between the seismic ray path and foliation plane of Cuba serpentinite at room *P* and *T* (Bezacier et al., 2010).

icant in the flat-slab region away from the shallowly-dipping portion near the trench, where a significant portion of fluids appear to be released (Manea and Manea, 2011). Nevertheless, anomalously low shear speed (2.4–3.4 km/s) continues in the layer directly below the upper-plate crust (Fig. 2A). In fact, these seismic velocities are far lower than expected for unaltered Mid-Ocean Ridge Basalt (MORB) or gabbro in the appropriate region of pressure (P)–temperature (T) space (Hacker et al., 2003). The candidate mineral phase talc (a low-strength hydrous mineral) was proposed to match the properties of the low-velocity anomaly at constant ~45 km depth and a range of likely temperatures (500–800 °C) (Fig. 2D; Kim et al., 2010). The observed V_p/V_s values at the depth of the flat slab are 2.05 ± 0.25 (Fig. 2D; Kim et al., 2010).

There are alternative models for the origin of low velocity in this layer. For example, the addition of fluids along normal faults at the outer-rise of the incoming plate offshore of central Mexico (e.g., Ranero et al., 2003) could cause elevated pore fluid pressure (e.g., Christensen, 1984). Also, crack anisotropy (Wang et al., 2012) within the layer might contribute to observed low shear speeds and high V_p/V_s (Fig. 2C; Kim et al., 2010). These may help lower the velocities but are not sufficient by themselves without extreme amount of water or crack density. Note there are almost no sediments along this part of the Middle America Trench to contribute fluids to the subducting system (Currie et al., 2002). This is an important constraint because in southern Alaska subduction zone, low velocities (~20–40% reduction in V_s) are observed in the shallow-dipping subduction channel, and may be due to highly-sheared, fluid-saturated sediments from the trench in combination with elevated pore fluid pressure in the channel (Kim et al., submitted for publication). On the other hand, the effect of metasediments are not considered in the V_p/V_s-porosity compilation of Peacock et al. (2011) in Cascadia.

The presence of frictionally weak phases such as serpentine and talc in hydrated peridotites at the slab–mantle interface has been reported from a number of subduction zones (e.g., Wang et al., 2009). However, the occurrence of talc at the depth expected for the upper oceanic crust in the flat slab regime in central Mexico (Kim et al., 2010) is enigmatic and may provide important constraints in slab dip evolution and the dynamics of the flat-slab system, which is not yet understood based on the geologic and tectonic data (Nieto-Samaniego et al., 2006; Morán-Zenteno et al., 2007). In this paper, we link available geophysical, mineralogical, and petrological constraints to examine causes for the genesis of talc in the flat-slab region, and discuss its critical role in subduction dynamics during the slab flattening process.

2. Previous data and interpretations

The Cocos plate subducting beneath central Mexico is young (~16 My at the Middle America trench; Pardo and Suárez, 1995), but is relatively cold among the 'warm-slab' subduction systems due to lack of insulating sedimentary cover atop the subducting plate (Currie et al., 2002). A sedimentary sequence 170 m thick was recovered at DSDP Site 487 on the Cocos plate at 99°09′W and 15°51′N (cyan circle, Fig. 1), including ~100 m of continentally derived Quaternary hemipelagic sediments that overlie late Miocene–Pliocene pelagic sediments (Watkins et al., 1982). Beneath this sedimentary cover, fragments of altered oceanic crust from Site 487 are mainly composed of an olivine- and plagioclase-bearing basalt (Verma, 2000). Previous seismic-refraction profiles at the trench near Acapulco (yellow line, Fig. 1) suggested 7–8 km of oceanic crust, which includes a sedimentary layer (Layer 1, P-wave velocity, $V_p = 2.15$ km/s), basement of 1.3 km (Layer 2, $V_p = 5.74$ km/s), and main crustal layer of 5.2 km (Layer 3, $V_p = 6.75$ km/s) (Shor and Fisher, 1961). Also, there might be bending-related extensional faults in the subducting crust offshore, which may provide pervasive pre-subduction hydration of the crust, as evidenced by multichannel seismic reflection images across Middle America trench slope offshore of Nicaragua in Central America (Ranero et al., 2003).

A recent onshore passive seismic experiment (MASE; Fig. 1) was carried out with the main purpose of imaging the subduction structure beneath central Mexico where the slab is poorly defined. The images obtained from the MASE data show the Cocos oceanic crust, which subducts (1) shallowly at an angle of 15° from ~75 km (the first seismic station is at Acapulco) to 150 km from the trench, and (2) horizontally to ~300 km from the trench at a depth of ~45 km. The low shear speed layer atop the oceanic crust is in direct contact with continental crust material (Fig. 2; Perez-Campos et al., 2008; Kim et al., 2010, 2012a), and the seismic velocity variations along the subduction plate interface clearly outline the seaward (up-dip) and landward (down-dip) limits of the seismogenic zone. Seismic stations near the Pacific coast show a smaller S wave velocity contrast at the base of the overlying crust in the strongly-coupled (locked) seismogenic zone (Song and Kim, 2012), where earthquakes are mostly concentrated (green dots, Fig. 2A). Such contrast abruptly increases toward the north where the stations sample the transition zone where slow-slip events (SSEs) predominantly occur (Song and Kim, 2012) and where there is an absence of large-magnitude earthquakes. In this transition zone and beyond (called "freely slipping zone" Kostoglodov et al., 2010), anomalously low shear speeds (2.4–3.4 km/s) are observed below the continental crust within a layer 4 ± 1 km thick (Fig. 2C; Song et al., 2009; Kim et al., 2010), interpreted as relict serpentinized mantle and/or altered oceanic crust (Perez-Campos et al., 2008; Kim et al., 2010). In the freely slipping zone, several regions of non-volcanic tremors (NVTs) have been identified above the flat slab (Fig. 2A; Payero et al., 2008), where strong dehydration occurs (Manea and Manea, 2011), and also the hydrous mineral talc is proposed to explain extremely low seismic velocities (Kim et al., 2010).

The converted amplitude of the thin low-velocity oceanic crust decreases significantly where the Cocos slab starts to bend downward at the southern edge of the volcanic arc at a lateral distance of 300 km from the trench and at a depth of 45–60 km (Kim et al., 2012a). Bayesian inversion of amplitudes in this zone yielded shear speeds ranging between 3.8 km/s and 4.3 km/s and V_p/V_s between 1.83 and ~2.0; such values may indicate the presence of hydrous minerals in combination with high pore pressure (Kim et al., 2012b). However, beyond 60 km and deeper, calculated velocities are much higher than predicted velocities for talc (Kim et al., 2012b).

For the "normal"-dipping subduction zone in southern Mexico, results from the other passive experiment in the Isthmus of Tehuantepec (only ~500 km southeast from MASE) reveal higher velocities for the subducted Cocos crust, indicating an amphibole-bearing oceanic crustal assemblage (Kim et al., 2012b). This makes the occurrence of talc beneath central Mexico more unusual and unique; it is apparently limited to the flat-slab environment.

Despite the long flat-slab segment with no intervening asthenosphere, both tectonic and past magmatic episodes indicate a lack of structural features and compression within the overriding plate in the last 20 Ma (Nieto-Samaniego et al., 2006; Morán-Zenteno et al., 2007). The thin low velocity layer along the crust–slab interface appears to decouple the subducting plate from the overriding plate, as is also demonstrated in time-dependent numerical models for generating the current slab configuration (Manea and Gurnis, 2007). Such weak coupling across the subduction interface gives rise to negligible upper-plate deformation.

A distinct surficial manifestation from the subduction of the Rivera (to the NW from this study region) and Cocos plates beneath the North American plate is the Trans-Mexican Volcanic Belt (TMVB, Fig. 1). The TMVB includes a broad zone of volcanism that spans from west to east in Mexico and contains several discrete volcanic fields. Several MASE seismic stations were situated within the Quaternary Chichinautzin volcanic field, directly south of Mexico City, which contains numerous cinder cones, shield volcanoes, and stratovolcanoes such as Popocatépetl (white triangle, Fig. 1). Along the MASE transect, the southern end of the current arc begins about 300 km from the trench, overlying the position where the slab subducts into the asthenosphere at the steep angle of ~75 degrees (Fig. 2A; Husker and Davis, 2009; Kim et al., 2010, 2012a). The top of the subducted slab at the start of the arc is at no more than ~100 km depth, based on the seismic images. A northward jump in the location of the volcanic arc in the early-middle Miocene constrains the timing of the transition in slab configuration from "normal" to flat (Ferrari et al., 1999). The flat slab reached a maximum extent of ~450 km from the trench at ~10 Ma before the onset of rollback, as indicated by trenchward migration of volcanism at a rate of ~10 km/Myr (Ferrari, 2004). Prominent low-conductivity zones in lower continental crust imaged by magnetotelluric survey (Jödicke et al., 2006), high seismic attenuation (Chen and Clayton, 2009), and low shear wave velocities (Iglesias et al., 2010) support past episodes of delivery of slab-derived fluids into the continental crust as the slab rolled back.

3. Generation of talc in the Cocos subduction system

The free-air gravity over the Middle America trench suggests that the primary source of sediments in the subduction process is the scraping of unconsolidated pelagic sediments from the top of the subducting oceanic plate (Manea et al., 2003). The terrigenous sediment contribution to the subducted crust is suggested to be minimal (Manea et al., 2003) and, as discussed earlier, the sedimentary column (Layer 1) at the top of the basaltic oceanic crust (Layers 2 and 3) is very thin near the trench (Currie et al., 2002). Also, high pore fluid pressure may explain observed seismic anomalies (low velocities, high V_p/V_s, and occurrence of slow slip earthquake) in very localized regions along the MASE profile, in the shallow-dipping upper portion of crust (Song and Kim, 2012). The hydrated metabasaltic oceanic crust subducts at the trench, subsequently undergoes subduction-zone metamorphism, and continues to release H_2O via dehydration reactions (Manea and Manea, 2011).

Strong negative and positive amplitude signals in the receiver functions at the top and bottom of the horizontal slow layer, respectively, beneath continental Moho at constant pressure (Fig. 2B), provide constraints on the velocity changes across the interfaces. Modeled seismic velocities (V_s and V_p/V_s) have been compared to seismic velocities computed for candidate slab mineralogies (Kim et al., 2010). Here, the V_p/V_s was computed with a fixed V_p of 5.54 km/s (Kim et al., 2010), which is similar to the V_p used to fit seismic waveforms recorded from nearby stations in central Mexico to map out the lateral extent of the very slow velocities (Dougherty et al., 2012). A large concentration of the hydrous mineral talc in the shallow and flat segment was proposed to reconcile the extremely low seismic velocities (Fig. 2D; Kim et al., 2010). There is in fact no lithology identified in the phase diagrams provided by Hacker et al. (2003), which are computed for the expected bulk compositions of the oceanic crustal layers, that can explain such low observed speeds. A drastic change in subducted crustal composition as a result of alteration and interaction with fluids and melts would be required to change mineral stability fields and allow greater hydration or the formation of talc and related minerals. However, such a case is considered to be unlikely based on models for the subduction system in central Mexico for the past 30 My (Ferrari et al., 2012). To generate such a low-velocity anomaly in the depth for the upper oceanic crust from typical crustal rocks would require an unreasonably high amount of free water (>~ 20 wt%) to reduce the velocities significantly (see Fig. 3). Preferentially oriented serpentinites, such as preferentially oriented antigorite, may provide an explanation to some of these sampled regions (Fig. 2D; Bezacier et al., 2010; Mookherjee and Capitani, 2011), but antigorite alone cannot be invoked to explain the full range of our observations (Kim et al., 2012b). Mookherjee and Capitani (2011) reported that both talc and antigorite may be responsible for trench parallel seismic anisotropy and large delay time at the base of the subduction zone mantle wedge.

Talc, in isolation, has a P–T range of stability that extends from surficial to eclogite-facies conditions, making it of potential significance in various faulting environments (Moore and Lockner, 2008). Because of its aseismic and thermally stable behavior (~800 °C at 1–2 GPa), talc may play a role in stabilizing slip at depth in the subduction zone (Moore and Lockner, 2008). Talc mainly forms as a result of the reaction of serpentine minerals with silica-saturated fluids liberated during dehydration of the subducting slab (Peacock and Hyndman, 1999; Moore and Rymer, 2007; Moore and Lockner, 2008), and may control the rheology of the slab–mantle interface (Hirauchi et al., 2012) and the down-dip limit of subduction-zone earthquakes (Peacock and Hyndman, 1999; Abers et al., 2006). Talc was found in the serpentinized peridotites collected from the landward trench slope of the southern Mariana forearc, and was used to explain observed low seismic velocities atop the plate interface and aseismic slip in the Izu–Bonin–Mariana subduction system (Wang et al., 2009). In addition, talc has been recently identified in the San Andreas fault, where it may explain the aseismic slip of the creeping section (Moore and Rymer, 2007).

Based on the P–T diagrams for depleted lherzolite and harzburgite with no free water, 11 vol% of talc atop the oceanic crust or 15 vol% beneath the oceanic crust can be present (Hacker et al., 2003). However, very little or almost no talc appears in the MORB composition phase diagram of Hacker et al. (2003) and indeed the P–T curves for equilibria involving talc based on available thermodynamic data (Deer et al., 1992) show that formation of talc in any basaltic composition is nearly impossible. Hence, for any metamorphosed basalt at the pressure of ~1.5 GPa (the depth of the flat slab in central Mexico), it takes an unreasonable amount of free water to obtain shear wave velocities sufficiently low to match the observed slow layer (Fig. 3). Fig. 3 also suggests that the only feasible way to generate the extremely low V_s observed in the flat-slab region is from altered mantle lithologies such as harzburgite, based on mineral physics data. Fig. 3C also shows that if a significant fluid fraction (<5%) of melt or free water is assumed to occur in the form of films of a certain aspect ratio (i.e. 0.01 for central Mexico), then the calculated seismic parameters agree well with the observed data. Free water requires the maintenance of impermeable fluid sealing along a 200 km interface that is shearing at a rate of 6 cm/yr (from EarthByte poles, Muller et al., 2008). The analysis by Peacock et al. (2011) for the Cascadia subduction zone argued that this is feasible but in that location sealing need only be maintained for a distance of a few kilometers but in central Mexico maintaining the seal over the 200 km length seems unlikely (Manea and Manea, 2011). The film geometry might be more appropriate than spheres, considering the highly sheared past deformation history in the region. Thus, with or without free fluid, a talc-rich ultramafic layer is required and the petrological evidence suggests that – even though this layer appears in the location expected for subducted upper oceanic crust – it must be generated from an ultramafic source derived from the mantle wedge rather

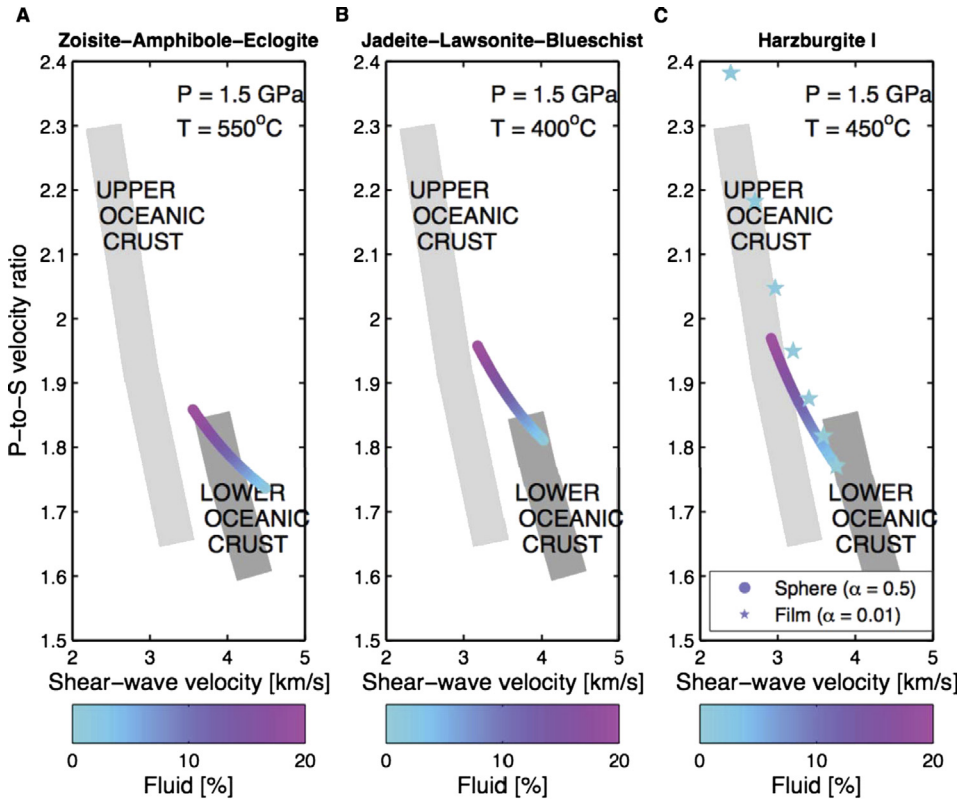

Fig. 3. Calculated V_p/V_s ratio versus V_s at a depth of 40–50 km for candidate rocks (A – Zoisite–Amphibole–Eclogite, B – Jadeite–Lawsonite–Blueschist, and C – Harzburgite I) considering free water from 0 to 20 wt%. The calculation of the seismic parameters with the free water component (sphere geometry with an aspect ratio α of 0.5 for all three rocks and also α of 0.01 for Harzburgite I) are based on Schmeling (1985) (see Kim et al., 2010, 2012b, for detailed references on the elastic parameters used). For each phase, the seismic velocities are computed according to slightly different temperatures at 1.5 GPa based on the stability fields suggested by Hacker et al. (2003). Light- and dark-gray shaded regions denote upper and lower oceanic crustal data considering different choices of V_p, respectively.

than from the trench. This inference is significant because there is no indication of a buoyant oceanic impactor (on the conjugate plate) that could have induced a flat-slab episode in central Mexico (Skinner and Clayton, 2010). Rather the presence of mantle-derived talc in the thin layer between slab and upper plate gives direct evidence that the slab dip evolution was due to changes in mantle wedge properties (vertical thickness, viscosity, and composition). The abundant occurrence of the mantle-derived minerals in the present-day subduction system probably would indicate that the mantle wedge had high H_2O concentration due to the dehydration of subducted sediments and oceanic crust, and that the mantle peridotite would react with slab fluids to form serpentinite and talc. Subsequently the mantle wedge viscosity is decreased, forming a low viscosity wedge on top of the subducting slab, which further facilitates into current state (Manea and Gurnis, 2007).

Thicknesses of the oceanic crust offshore of Mexico has been observed to be 7–8 km (Shor and Fisher, 1961). However, if the 4 ± 1 km thick (Song et al., 2009; Kim et al., 2010) extremely low-V_s layer is assigned to material derived from the mantle wedge such as talc and serpentine, then the remaining subjacent slow layer assigned to subducted oceanic crust along the flat segment is only 3–5 km (Figs. 2A and 2C). Even allowing that the 0.5–1.5 km sedimentary sequence observed in the offshore refraction line may not be present everywhere (only 170 m is present at DSDP Site 487) and may be accreted to the upper plate at the trench, the inferred layer of subducting oceanic crust is unexpectedly thin. Nevertheless, the assignment of the extremely low-V_s layer to mantle-wedge-derived material is supported by the observed oceanic crustal thickness at the up-dip termination of this layer in the shallowly subducting region. An abrupt change in S wave velocity contrast at the base of the overlying fore-arc crust is observed ~100 km from the trench (~25 km from the Pacific coast) (Fig. 2A; Song and Kim, 2012). This point separates the region between the deep locked zone and transition zone, and the deep locked zone appears to have normal oceanic crustal velocity (Song and Kim, 2012), which suggests no influence from the mantle wedge.

4. Influence of talc on subduction dynamics

Integrating geophysical, petrological, and mineralogical observations, we suggest the following sequence of events (Miocene to present) for the evolution of the slab flattening process:

1. Prior to ~25 Ma, the Cocos plate beneath central Mexico was in "normal" configuration (Ferrari et al., 2012). Trench-parallel Miocene magmatic arc was positioned at ~100 km from the trench.

2. From 25 to 10 Ma (Ferrari et al., 2012, and references therein), the progressive flattening of the Cocos plate occurred, for reasons that remain unknown, and the magmatic arc migrated inland to the northern edge of the TMVB. In this period, the upper surface of the Cocos plate was brought into contact with the base of the overlying plate and, as a consequence, the low-density asthenosphere was squeezed out in the direction of subduction. Active dehydration of the downgoing Cocos slab resulted in (a) hydration of the North American mantle lithosphere, and (b) decrease in the viscosity on top of the subducting slab, thus creating the low-viscosity channel (Manea and Gurnis, 2007). The numerical models require a narrow range ($5–10 \times 10^{19}$ Pa s) of mantle viscosities to produce the present flat-slab configuration, consistent with seismic results (e.g., Perez-Campos et al., 2008). Due to cooling caused by the displacement of the mantle corner flow and

the passage of cold oceanic lithosphere beneath the trapped overriding lithosphere, the mantle material above the flat slab was not hot enough to form melt, and will instead produce hydrous minerals like serpentine and talc. The presence of these weak minerals in the wedge induced flow, which then increased suction and flatten the slab (Manea and Gurnis, 2007).

3. Circa 10 Ma (Manea et al. 2013a, 2013b), the volcanism proceeded to migrate southward to its present location just south of Mexico City due to slab rollback (Ferrari, 2004). This slab-rollback process allows the hot mantle wedge to flow back into the newly created space, which also initiates southward migration of volcanism. The broad, elongated low-resistivity region imaged in the lower crust beneath the TMVB by a magnetotelluric experiment (Jödicke et al., 2006) shows direct evidence of the past and continuous subducting slab dehydration and its rollback.

A large extent and heterogeneous volcanic signatures in the TMVB have been suggested to be due to a change in subduction dynamics from normal subduction geometry to the current configuration (Blatter et al., 2007; Johnson et al., 2009). In particular, high mantle H_2O concentrations (0.3–0.7 wt%) beneath most parts of the arc near the MASE profile suggest that H_2O in the mantle source: (1) is partly contained in hydrous minerals or in a fluid or hydrous melt phase (or both), (2) lowers the melting temperature, and (3) is the result of fluids or hydrous melts from the subducted slab (Johnson et al., 2009). Whereas, the occurrence of low-H_2O melts (far behind the volcanic front) is due to extension-related decompression melting with little input of slab-derived fluids (Blatter et al., 2007; Johnson et al., 2009). This can be explained by corner-flow-driven advection of mantle from behind the arc (Blatter et al., 2007; Johnson et al., 2009), which correlates well with the subduction dynamics model for central Mexico.

The case of central Mexico is enigmatic because of the lack of apparent causes of the slab flattening. Although the flat subduction of the Cocos plate is clear, its origin is not apparent because neither a buoyant subducted oceanic lithosphere impactor nor its conjugate on the Pacific plate can be found (Skinner and Clayton, 2010). Furthermore, the presence of talc-rich assemblage in the flat upper oceanic crust is unusual (Kim et al., 2010). Our analysis suggests that talc has to come from the mantle wedge based on the phase equilibria involving talc. The formation of talc-rich assemblages under upper oceanic crustal depth conditions are likely to represent a portion of the remnant mantle wedge that has been pinched by the slab as the dip angle shallowed (Manea and Gurnis, 2007). Its effect on the current system gives rise to unusually low shear velocities (Song et al., 2009; Kim et al., 2010), seismic anisotropy (Song and Kim, 2012), and episodic tremor and slip (Payero et al., 2008; Kostoglodov et al., 2010). Also, its exceptionally weak frictional properties decouple the subducted slab from the overlying plate with no upper plate deformation.

5. Conclusions

The hydrous mantle mineral talc has been previously proposed to explain anomalously low shear wave speeds at the subducted (top) interface of the Cocos plate in central Mexico. This study suggests that this talc component comes from the mantle wedge rather than from the trench based on the stability field of talc at the depth of the flat slab. It was originally created from serpentines in hydrated peritodites in the mantle wedge during interaction with Si-saturated fluids via dewatering of the subducted slab. Our hypothesis is consistent with published time-dependent numerical models for generating the flat-slab configuration. The evolution of the thin low-velocity shear zone, enriched with low-strength talc, generated from the mantle wedge has significant implications for the subduction dynamics as well as the geochemistry of the mantle wedge and arc beneath the Trans-Mexican Volcanic Belt.

Acknowledgements

This work was funded by the Korea Meteorological Administration Research and Development Program under Grant CATER-2013-8010. This study was also supported by the Gordon and Betty Moore Foundation through the Tectonics Observatory at California Institute of Technology (Contribution number 223) and NSF award EAR 0609707. We used Excel Worksheets and Macros from Hacker and Abers (2004) for calculating seismic speeds. We thank Xyoli Perez-Campos, Arturo Iglesias, and others at the Universidad Nacional Autonoma de Mexico for deploying and maintaining the MASE line. We also thank Joann Stock and Michael Gurnis from California Institute of Technology for discussions. Finally, we thank Editor Peter Shearer, Pascal Audet, and one anonymous reviewer for helpful comments which improved the manuscript.

References

Abers, G.A., 2000. Hydrated subducted crust at 100–250 km depth. Earth Planet. Sci. Lett. 176, 323–330.

Abers, G.A., 2005. Seismic low-velocity layer at the top of subducting slabs: observations, predictions, and systematics. Phys. Earth Planet. Inter. 149, 7–29.

Abers, G.A., Plank, T., Hacker, B.R., 2003. The wet Nicaragua slab. Geophys. Res. Lett. 30 (2), http://dx.doi.org/10.1029/2002GL015649.

Abers, G.A., van Keken, P.E., Kneller, E.A., Ferris, A., Stachnik, J.C., 2006. The thermal structure of subduction zones constrained by seismic imaging: Implications for slab dehydration and wedge flow. Earth Planet. Sci. Lett. 241, 387–397.

Audet, P., Bostock, M.G., Christensen, N.I., Peacock, S.M., 2009. Seismic evidence for overpressured subducted oceanic crust and megathrust fault sealing. Nature 457, 76–78.

Bezacier, L., Reynard, B., Bass, J.D., Sanchez-Valle, C., Van de Moortele, B., 2010. Elasticity of antigorite, seismic detection of serpentinites, and anisotropy in subduction zones. Earth Planet. Sci. Lett. 289, 198–208, http://dx.doi.org/10.1016/j.epsl.2009.11.009.

Blatter, D.L., Lang Farmer, G., Carmichael, I.S.E., 2007. A north–south transect across the central Mexican volcanic belt at ~100°W: spatial distribution, petrological, geochemical, and isotopic characteristics of Quaternary volcanism. J. Petrol. 48 (5), 901–950, http://dx.doi.org/10.1093/petrology/egm006.

Chen, T., Clayton, R.W., 2009. Seismic attenuation structure in central Mexico: Image of a focused high-attenuation zone in the mantle wedge. J. Geophys. Res. 114, B07304, http://dx.doi.org/10.1029/2008JB005964.

Christensen, N.I., 1984. Pore pressure and oceanic crustal seismic structure. Geophys. J. R. Astron. Soc. 79, 411–423.

Christensen, N.I., 1989. Pore pressure seismic velocities, and crustal structure. In: Pakiser, L.C., Mooney, W.D. (Eds.), Geophysical Framework of the Continental United States. In: Geol. Soc. Am. Mem., vol. 172, pp. 783–798.

Christensen, N.I., Salisbury, M.H., 1975. Structure and constitution of the lower oceanic crust. Rev. Geophys. Space Phys. 13, 57–86, http://dx.doi.org/10.1029/RG013i001p00057.

Currie, C.A., Hyndman, R.D., Wang, K., Kostoglodov, V., 2002. Thermal models of the Mexico subduction zone: Implications for the megathrust seismogenic zone. J. Geophys. Res. 107, B12, http://dx.doi.org/10.1029/2001JB000886.

Deer, W.A., Howie, R.A., Zussman, J., 1992. An Introduction to the Rock-Forming Minerals, 2nd ed. Longman Scientific & Technical.

Dougherty, S., Clayton, R.W., Helmberger, D.V., 2012. Seismic structure in central Mexico: Implications for fragmentation of the subducted Cocos plate. J. Geophys. Res. 117, B09316, http://dx.doi.org/10.1029/2012JB009528.

Ferrari, L., 2004. Slab detachment control on mafic volcanic pulse and mantle heterogeneity in central Mexico. Geology 32, 77–80, http://dx.doi.org/10.1130/G19887.1.

Ferrari, L., Lopez-Martinez, M., Aquirre-Diaz, G., Carrasco-Niunez, G., 1999. Space–time patterns of Cenozoic arc volcanism in central Mexico: From the Sierra Madre Occidental to the Mexican Volcanic Belt. Geology 27 (4), 303–306.

Ferrari, L., Orozco-Esquivel, T., Manea, V., Manea, M., 2012. The dynamic history of the Trans-Mexican Volcanic Belt and the Mexico subduction zone. Tectonophysics 522–523, 122–149.

Gephart, J.W., 1994. Topography and subduction geometry in the central Andes: clues to the mechanics of a noncollisional orogeny. J. Geophys. Res. 99 (B6), 12279–12288, http://dx.doi.org/10.1029/94JB00129.

Gutscher, M.-A., Spakman, W., Bijwaard, H., Engdahl, E.R., 2000. Geodynamics of flat subduction: Seismicity and tomographic constraints from the Andean margin. Tectonics 19, 814–833, http://dx.doi.org/10.1029/1999TC001152.

Hacker, B.R., Abers, G.A., 2004. Subduction Factory 3: An Excel worksheet and macro for calculating the densities, seismic wave speeds, and H_2O contents of minerals and rocks at pressure and temperature. Geochem. Geophys. Geosyst. 5, 1, http://dx.doi.org/10.1029/2003GC000614.

Hacker, B.R., Abers, G.A., Peacock, S.M., 2003. Subduction Factory 1. Theoretical mineralogy, densities, seismic wave speeds, and H_2O contents. J. Geophys. Res. 108, 1–26.

Hansen, R.T., Bostock, M.G., Christensen, N.I., 2012. Nature of the low velocity zone in Cascadia from receiver function waveform inversion. Earth Planet. Sci. Lett. 337–338, 25–38.

Hirauchi, K.-I., den Hartog, S.A.M., Spiers, C.J., 2012. Weakening of the slab–mantle wedge interface induced by metasomatic growth of talc. Geology 41 (1), http://dx.doi.org/10.1130/G33552.1.

Husker, A., Davis, P.M., 2009. Tomography and thermal state of the Cocos plate subduction beneath Mexico City. J. Geophys. Res. 114, B04306, http://dx.doi.org/10.1029/2008JB006039.

Iglesias, A., Clayton, R.W., Perez-Campos, X., Singh, S.K., Pacheco, J.F., Garcia, D., Valdes-Gonzalez, C., 2010. S wave velocity structure below central Mexico using high-resolution surface wave tomography. J. Geophys. Res. 115, B06307, http://dx.doi.org/10.1029/2009JB006332.

Jödicke, H., Jording, A., Ferrari, L., Arzate, J., Mezger, K., Rupke, L., 2006. Fluid release from the subducted Cocos plate and partial melting of the crust deduced from magnetotelluric studies in southern Mexico: Implications for the generation of volcanism and subduction dynamics. J. Geophys. Res. 111, B08102, http://dx.doi.org/10.1029/2005JB003739.

Johnson, E.R., Wallace, P.J., Granados, H.D., Manea, V.C., Kent, A.J.R., Bindeman, I.N., Donegan, C.S., 2009. Subduction-related volatile recycling and magma generation beneath central Mexico: insights from melt inclusions, oxygen isotopes and geodynamic models. J. Petrol. 50 (9), 1729–1764.

Kim, Y., Abers, G.A., Li, J., Christensen, D., Calkins, J., Rondenay, S., submitted for publication. Alaska Megathrust 2: Imaging the megathrust zone and Yakutat/Pacific plate interface in the Alaska subduction zone. 2013.

Kim, Y., Clayton, R.W., Jackson, J.M., 2010. Geometry and seismic properties of the subducting Cocos plate in central Mexico. J. Geophys. Res. 115, B06310, http://dx.doi.org/10.1029/2009JB006942.

Kim, Y., Clayton, R.W., Jackson, J.M., 2012b. Distribution of hydrous minerals in the subduction system beneath Mexico. Earth Planet. Sci. Lett. 341–344, 58–67.

Kim, Y., Miller, M.S., Pearce, F.D., Clayton, R.W., 2012a. Seismic imaging of the Cocos plate subduction zone system in central Mexico. Geochem. Geophys. Geosyst. 13, Q07001, http://dx.doi.org/10.1029/2012GC004033.

Kodaira, S., Iidaka, T., Kato, A., Park, J.O., Iwasaki, T., Kaneda, Y., 2004. High pore fluid pressure may cause silent slip in the Nankai trough. Science 304, 1295–1298, http://dx.doi.org/10.1126/science.1096535.

Kostoglodov, V., Huster, A., Shapiro, N.M., Payero, J.S., Campillo, M., Cotte, N., Clayton, R., 2010. The 2006 slow slip event and nonvolcanic tremor in the Mexican subduction zone. Geophys. Res. Lett. 37, L24301, http://dx.doi.org/10.1029/2010GL045424.

Lallemand, Heuret, S.A., Boutelier, D., 2005. On the relationships between slab dip, back-arc stress, upper plate absolute motion, and crustal nature in subduction zones. Geochem. Geophys. Geosyst. 6, Q09006, http://dx.doi.org/10.1029/2005GC000917.

Larson, K., Kostoglodov, V., Miyazaki, S., Santiago, J.A.S., 2007. The 2006 aseismic slow slip event in Guerrero, Mexico: New results from GPS. Geophys. Res. Lett. 34, L13309, http://dx.doi.org/10.1029/2007GL029912.

Lay, T., Bilek, S.L., 2007. Anomalous earthquake ruptures at shallow depths on subduction zone megathrusts. In: Dixon, T., Moore, C. (Eds.), The Seismogenic Zone of Subduction Thrust Faults. Columbia University Press, pp. 476–511.

Mainprice, D., Le Page, Y., Rodgers, J., Jouanna, P., 2008. Ab initio elastic properties of talk from 0 to 12 GPa: Interpretation of seismic velocities at mantle pressures and prediction of auxetic behaviour at low pressure. Earth Planet. Sci. Lett. 274, 327–338, http://dx.doi.org/10.1016/j.epsl.2008.07.047.

Manea, V.C., Gurnis, M., 2007. Subduction zone evolution and low viscosity wedges and channels. Earth Planet. Sci. Lett. 264, 22–45.

Manea, V.C., Manea, M., 2011. Flat-slab thermal structure and evolution beneath central Mexico. Pure Appl. Geophys. 168, 1475–1487, http://dx.doi.org/10.1007/s00024-010-0207-9.

Manea, V.C., Manea, M., Ferrari, L., 2013a. A geodynamical perspective on the subduction of Cocos and Rivera plates beneath Mexico and Central America. Tectonophysics 522–523, 122–149, http://dx.doi.org/http://dx.doi.org/10.1016/j.tecto.2012.12.039.

Manea, M., Manea, V.C., Kostoglodov, V., 2003. Sediment fill in the Middle America Trench inferred from gravity anomalies. Geofís. Int. 42, 603–612.

Manea, V.C., Perez-Gussinye, Manea, M., 2013b. Chilean flat slab subduction controlled by overriding plate thickness and trench rollback. Geology 40, 35–38, http://dx.doi.org/10.1130/G32543.1.

Marschall, H.R., Schumacher, J.C., 2012. Arc magmas sourced from mélange diapirs in subduction zones. Nat. Geosci. 5, 862–867, http://dx.doi.org/10.1038/NGEO1634.

MASE. 2007. Meso America Subduction Experiment. Caltech. Dataset. http://dx.doi.org/10.7909/C3RN35SP.

Mookherjee, M., Capitani, G.C., 2011. Trench parallel anisotropy and large delay times: Elasticity and anisotropy of antigorite at high pressures. Geophys. Res. Lett. 38, L09315, http://dx.doi.org/10.1029/2011GL047160.

Moore, D.E., Lockner, D.A., 2008. Talc friction in the temperature range 25°–400°C: Relevance for fault-zone weakening. Tectonophysics 449, 120–132.

Moore, D.E., Rymer, M.J., 2007. Talc, serpentinite, and the creeping section of the San Andreas fault. Nature 448, 795–797.

Morán-Zenteno, D.J., Cerca, M., Keppie, J.D., 2007. The Cenozoic tectonic and magmatic evolution of southwestern Mexico: Advances and problem interpretation. In: Alaniz-Álvarez, S.A., Nieto-Samanieto, Á.F. (Eds.), Geology of Mexico, Celebrating the Centenary of the Geological Society of Mexico. In: Spec. Pap., Geol. Soc. Am., vol. 422, pp. 71–91.

Muller, R.D., Sdrolias, M., Gaina, C., Roest, W.R., 2008. Age, spreading rates, and spreading asymmetry of the world's ocean crust. Geochem. Geophys. Geosyst. 9, Q04006, http://dx.doi.org/10.1029/2007GC001743.

Nieto-Samaniego, A.F., Alaniz-Álvarez, A.S., Silva-Romo, G., Eguiza-Castro, M.H., Mendoza-Rosales, C., 2006. Latest Cretaceous to Miocene deformation events in the eastern Sierra Madre del Sur, Mexico, inferred from the geometry and age of major structures. Geol. Soc. Am. Bull. 118, 238–252, http://dx.doi.org/10.1130/B25730.1.

Pardo, M., Suárez, G., 1995. Shape of the subducted Rivera and Cocos plates in southern Mexico: Seismic and tectonic implications. J. Geophys. Res. 100 (B7), 12,357–12,373, http://dx.doi.org/10.1029/95JB00919.

Payero, J.S., Kostoglodov, V., Shapiro, N., Mikumo, T., Iglesias, A., Pérez-Campos, X., Clayton, R.W., 2008. Nonvolcanic tremor observed in the Mexican subduction zone. Geophys. Res. Lett. 35, L07305, http://dx.doi.org/10.1029/2007GL032877.

Peacock, S.M., Christensen, N.I., Bostock, M.G., Audet, P., 2011. High pore pressures and porosity at 35 km depth in the Cascadia subduciton zone. Geology 470–474, http://dx.doi.org/10.1130/G31649.1.

Peacock, S.M., Hyndman, R.D., 1999. Hydrous minerals in the mantle wedge and the maximum depth of subduction thrust earthquakes. Geophys. Res. Lett. 26 (16), 2517–2520.

Perez-Campos, X., Kim, Y., Husker, A., Davis, P.M., Clayton, R.W., Iglesias, A., Pacheco, J.F., Singh, S.K., Manea, V.C., Gurnis, M., 2008. Horizontal subduction and truncation of the Cocos Plate beneath central Mexico. Geophys. Res. Lett. 35, 18.

Perez-Gussinye, M., Lowry, A.R., Phipps Morgan, J., Tassara, A., 2008. Effective elastic thickness variations along the Andean margin and their relationship to subduction geometry. Geochem. Geophys. Geosyst. 9, http://dx.doi.org/10.1029/2007GC001786.

Ranero, C.R., Phipps Morgan, J., Mcintosh, K., Reichert, C., 2003. Bending-related faulting and mantle serpentinization at the Middle America trench. Nature 425, 367–373.

Schmeling, H., 1985. Numerical models on the influence of partial melt on elastic, anelastic and electric properties of rocks. Part I: elasticity and anelasticity. Phys. Earth Planet. Inter. 41, 34–57.

Shelly, D.R., Beroza, G.C., Ide, S., Nakamula, S., 2006. Low-frequency earthquakes in Shikoku, Japan, and their relationship to episodic tremor and slip. Nature 442, 188–191.

Shor, G.G., Fisher, R.L., 1961. Middle America Trench: Seismic-refraction studies. Geol. Soc. Am. Bull. 72, 721–730.

Skinner, S.M., Clayton, R.W., 2010. An evaluation of proposed mechanisms of slab flattening in central Mexico. Pure Appl. Geophys. 168, 1461–1474, http://dx.doi.org/10.1007/s00024-010-0200-3.

Song, T.A., Helmberger, D.V., Brudzinski, M.R., Clayton, R.W., Davis, P., Perez-Campos, X., Singh, S.K., 2009. Subducting slab ultraslow velocity layer conincident with silent earthquake in southern Mexico. Science 324, 502–506.

Song, T.A., Kim, Y., 2012. Localized seismic anisotropy associated with long-term slow-slip events beneath southern. Mexico. Geophys. Res. Lett. 39, L09308, http://dx.doi.org/10.1029/2012GL051324.

Verma, S., 2000. Geochemistry of the subducting Cocos plate and the origin of subduction-unrelated mafic volcanism at the front of the central Mexican Volcanic Belt. In: Delgado-Granados, H., Aguirre-Diaz, G., Stock, J. (Eds.), Cenozoic Tectonics and Volcanism of Mexico. In: Spec. Pap., Geol. Soc. Am., vol. 334, pp. 1–28.

Wang, X.-Q., Schubnel, A., Fortin, J., David, E.C., Gueguen, Y., Ge, H.-K., 2012. High V_p/V_s ratio: Saturated cracks or anisotropy effects?. Geophys. Res. Lett. 39, L11307, http://dx.doi.org/10.1029/2012GL051742.

Wang, X., Zeng, Z., Liu, C., Chen, J., Yin, X., Wang, X., Chen, D., Zhang, G., Chen, S., Li, K., Ouyang, H., 2009. Talc-bearing serpentinized peridotites from the southern Mariana forearc: Implications for aseismic character within subduction zones. Chin. J. Oceanol. Limnol. 27 (3), 667–673.

Watkins, J.S., Moore, J.C., Niitsuma, N., 1982. Initial Reports of the Deep Sea Drilling Project, vol. 66. U.S. Government Printing Office. 864 pp.